ORIGINAL PAPER

Bearing Capacity Characteristic Analysis of Anti-floating Bolts in Unsaturated Soil Based on Mindlin Solution

Xu Fu[1] · Qian LI[1] · Huanqin Liu[1] · Lintai Wang[1] ·
Xiaoli Liu[1]

Abstract Based on Mindlin solution and the theory of unsaturated soil mechanics, the theoretical solutions of shear stress and axial force distribution in the elastic stage of full-length binding-type anti-floating bolts were derived, and the bearing capacity characteristics of such bolts and the influencing factors were analyzed. In this paper, the design parameters of anti-floating anchor in a negative two-floor basement of a commercial square are substituted into the formula derived in this paper. The results show that, in unsaturated soil, the shear stress and axial force of the full-length bonded anti-floating anchor are distributed along the total length of the anchor, but neutral points appear in both of them, which is mainly due to the reduction of the axial force and shear stress of the anti-floating anchor caused by the matric suction. The formula derived in this paper is used to analyze the factors affecting the bearing capacity of anti-floating anchor bolt in unsaturated soil. The results show that: the greater the elastic modulus of soil mass, the greater the peak value of shear stress curve, the closer the peak value is to the head of anchor bolt, and the greater the axial force decline rate. With the increase of anchor solid diameter D, the peak value of shear stress decreases, the peak value moves backward, the neutral point moves forward, the negative shear stress value increases, the decline rate of axial force distribution curve decreases, but the negative axial force increases. With the increase of the additional shear stress τ_0, the peak value of the shear stress curve decreases, the peak value moves to the hole of the anchor rod, the neutral point moves to the hole, the negative shear stress increases, the decline rate of the axial force distribution curve increases, and the negative axial force increases.

Keywords Anti-floating bolt · Unsaturated soil · Mindlin solution · Stress analysis · Influencing factors

Introduction

The inland areas in North China are mostly arid or semi-arid, and most shallow soil encountered in engineering practice is unsaturated soil, which is solid, liquid, and gas in three-phase medium, with more complex engineering characteristics than saturated soil due to the suction. [1–3] In recent years, the development and utilization of underground space has gradually increased. As the main medium for bearing the self-weight of underground structures, rock and soil bodies contain a large number of pores and fissures, including groundwater that will exert buoyancy on the foundation of buildings. When it exceeds the self-weight of the structure, it will cause structural deformation, cracking, and even damage to the entire building, resulting in serious economic losses and social impacts to the people and the country. In addition, due to the increasing frequency of extreme weather in today's world, many cities have experienced a regional rise in groundwater levels, which also leads to an increase in buoyancy of groundwater. The resulting buoyancy hazard cannot be ignored, and anti-floating design and corresponding anti-floating measures need to be adopted before construction to avoid the occurrence of such engineering problems. [4, 5] Anti-floating engineering mainly refers to the general term for engineering activities such as investigation, design, construction, testing and monitoring, and reinforcement to ensure the stability of the building's underground structure against floating. In the

✉ Xu Fu
fuxu431@163.com

1 College of Architectural Engineering, North China Institute of Aerospace Engineering, Langfang 065000, China

field of anti-floating engineering, the most commonly used anti-floating methods are: weighting method, drainage and water-separating decompression method, water discharge and decompression method, and anchoring method (anti-pulling pile and anti-floating anchor).

Anchor bolt is a tension rod embedded deep in rock and soil, which is usually called anti-floating anchor when it is used to resist the buoyancy of groundwater. The anchoring end of the anti-floating anchor bolt is generally buried in the bottom plate of the underground structure, and the anchor solid is buried in the rock and soil body. When the ground water buoyancy borne by the bottom plate of the underground structure increases, the anti-buoyancy force will be applied to the anti-buoyancy anchor rod through the anchoring end. At this time, the anchorage solid resists the uplift force through the friction resistance generated between the anchor and the surrounding rock and soil body to ensure the stability of the underground structure.

The anti-floating anchor can be divided into the following types: the full-length viscous anchor, the tensile anchor (pre-stressed anchor, scattered pre-stressed anchor), the pressure anchor (pre-stressed anchor, scattered pre-stressed anchor), and the enlarged end anchor. The anchor that is filled with viscous material along the whole length of the anchor rod is called the full-length viscous anchor, which is suitable for rock or soil layers. The tensile pre-stressed anchor is suitable for hard rocks and medium hard rocks. The tensile scattered pre-stressed anchor is suitable for soft rocks or soil layers. The pressure pre-stressed anchor is suitable for rock or soil layers with high corrosion resistance. The pressure scattered pre-stressed anchor is suitable for soft rocks and soil layers or rock and soil layers with high corrosion resistance. The enlarged end anchor is only applicable to soil layer. The full-length viscous anchor has the advantages of simple construction and low cost, and has been widely used. The structure diagram of the full-length bonded anti-floating anchor is shown in Fig. 1, and the design method is shown in Fig. 2. There are three main layout methods of anti-floating anchor, namely planar uniform layout, planar uniform layout, and plum blossom layout, as shown in Fig. 3.

Since traditional soil mechanics is mainly established for saturated soil, while unsaturated soil exists widely in nature, the real saturated soil exists less in nature. Therefore, the influence of matrix suction unique to unsaturated soil should be considered to solve the problem of bearing capacity of anti-floating anchors in unsaturated soil areas. Since the bearing capacity of anti-floating anchors depends on factors such as anchor deformation, surrounding rock and soil deformation, and interface load transfer, the deformation coordination relationship between the anchor and the rock and soil mass should be considered. The Mindlin solution can be applied to establish the deformation coordination relationship between the anchor and the rock and soil mass.
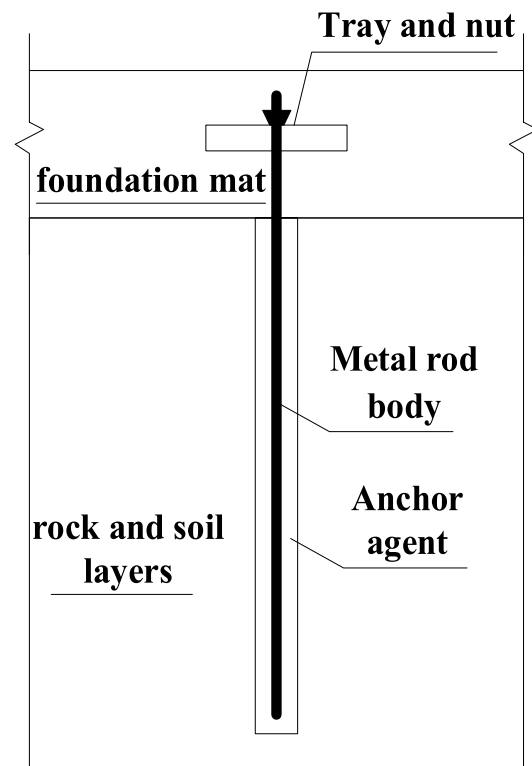
Fig. 1 Structure diagram of full-length bonded anti-floating anchor

At present, scholars at home and abroad have conducted a lot of theoretical and experimental work on the research of the bearing capacity characteristics of anti-floating anchor rods and the application of Mindlin solution in the field of geotechnics. Li et al. [6] develop a novel analytical model coupling the crack propagation in the grout annulus to capture the load–displacement performance of cable bolts under axial loading. Ma X et al. [7] deeply explored the action mechanism of full-length binding-type anti-floating bolts and its influencing factors, and deemed that the most common failure mode occurred at the interface between the anchoring body and surrounding rock. Jing D S et al. [8] carried out the pull-out failure test of anti-floating bolts, analyzed the failure load and displacement characteristics, and established the prediction equation for the bearing capacity. Liu G M [9] conducted field test and numerical simulation of the bearing capacity of full-length binding-type anti-floating bolts in strongly and moderately weathered sandstones, and results showed that the stress and displacement of the bolt at the upper part were much greater than those at the lower part, presenting a nonuniform distribution pattern.

Li et al. [10] developed an analytical model to simulate the load–displacement performance of rock bolts under axial loading based on modified continuously yielding criterion. Peng H et al. [11] established the stress distribution equation for the anchorage section of tensile-type

Fig. 2 Design method of full-length bonded anti-floating anchor

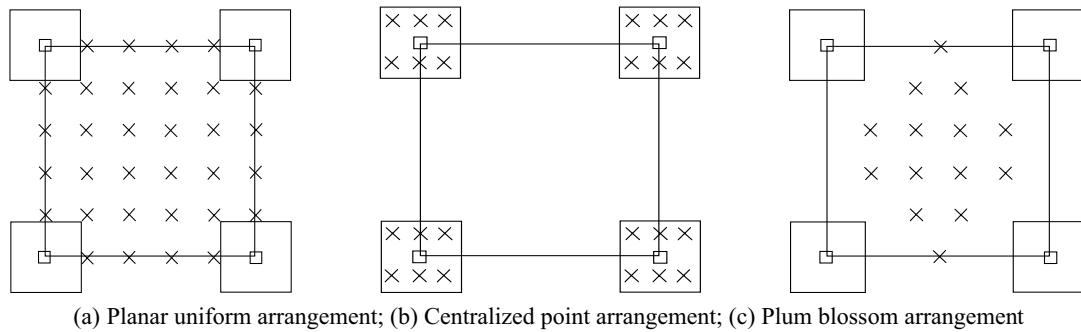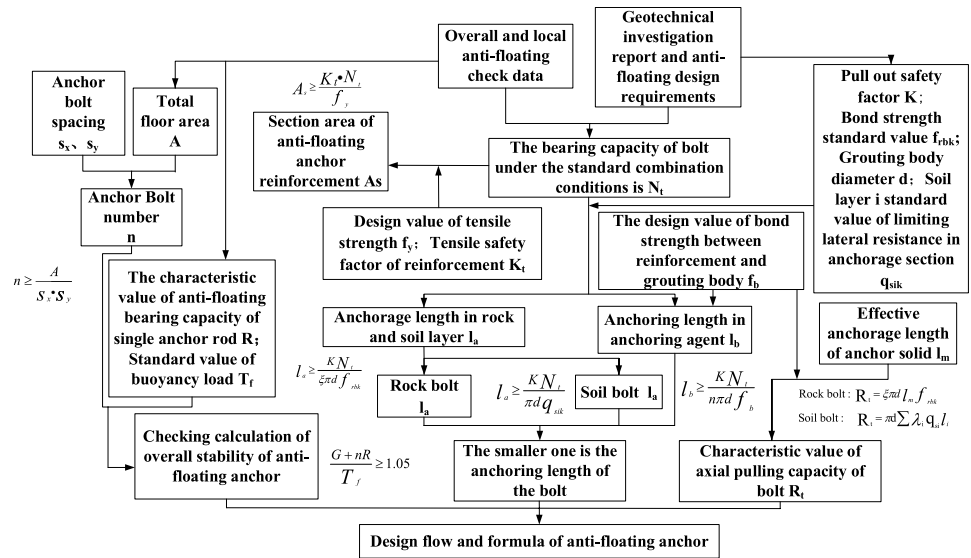(a) Planar uniform arrangement; (b) Centralized point arrangement; (c) Plum blossom arrangement

Fig. 3 Arrangement of anti-floating anchor

bolts and investigated the influencing factors. You C A [12] established the theoretical solution to the shear force distribution of full-length binding-type bolts along the bolt body based on the Mindlin solution and performed the stress analysis.

The above study results provide help and theoretical basis for determining the bearing capacity of anti-floating bolts, but the correlations of bearing capacity characteristics of full-length binding-type anti-floating bolts in unsaturated soil have been scarcely analyzed and discussed. Hence, the theoretical solutions to the shear stress and axial force distribution of full-length binding-type anti-floating bolts in the elastic stage were derived in this study based on the Mindlin solution and the theory of unsaturated soil mechanics. Then, the bearing capacity characteristics and influencing factors of such bolts were analyzed, thus providing a reference basis for anti-floating bolt design and calculation in unsaturated soil areas.

Elastic Solution to the Stress Distribution of Full-Length Binding-Type Anti-Floating Bolts

Mindlin Displacement Solution

The full-length binding-type anti-floating bolt is generally perpendicularly arranged in the unsaturated soil layer, with its ends subjected to the pull-out loading action, and the shear force is applied to the surrounding soil mass along the axial direction of the bolt. If the surrounding soil layer is regarded as a semi-infinite elastomer and the shear force as a concentrated force, this problem becomes an elastic problem where one point in the semi-infinite elastomer is subjected to a concentrated force, which can be analyzed via Mindlin displacement solution. [13, 14] The Mindlin displacement solution was derived by Professor Mindlin in 1936, with its mechanical model as shown in Fig. 4.
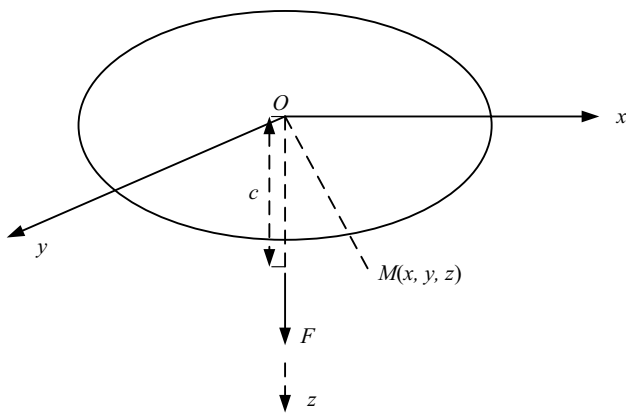
Fig. 4 Mechanical model of Mindlin displacement solution

As shown in Fig. 4, a concentrated force F acts upon a point c at the inner part of the linear-elastic and isotropic semi-infinite elastomer, and then the vertical displacement solution at M (x, y, z) is as follows:

$$W = \frac{F(1+\mu)}{8\pi E(1-\mu)} \left[\begin{array}{l} \dfrac{3-4\mu}{R_1} + \dfrac{8(1-\mu)^2 -(3-4\mu)}{R_2} + \\[2mm] \dfrac{(z-c)^2}{R_1^3} + \dfrac{(3-4\mu)(z+c)^2 -2cz}{R_2^3} + \\[2mm] \dfrac{6cz(z+c)^2}{R_2^5} \end{array} \right] \quad (1)$$

$$R_1 = \sqrt{x^2 + y^2 + (z-c)^2} \quad (2)$$

$$R_2 = \sqrt{x^2 + y^2 + (z+c)^2} \quad (3)$$

In Eq. (1), E and μ represent the elastic modulus and Poisson's ratio of the soil mass around the bolt, respectively.

At the plane origin, namely (0,0,0), the displacement caused by the concentrated force F at the position of (0,0,z) is expressed as below:

$$W(z) = \frac{F(1+\mu)(3-2\mu)}{2\pi Ez} \quad (4)$$

For the system composed of anti-floating anchor rods and surrounding rock and soil layers, the force F is the lateral friction between the anchor rods and the rock and soil layers. To facilitate the subsequent study, the following assumptions are made: (1) The soil mass and bolt are linear-elastic materials with the same properties; (2) the bolt is only subjected to a stress in the elastic stage; (3) the axial stress on the bolt's cross section is uniformly distributed; (4) at the plane origin, namely (0,0,0), the displacement of the soil mass at the plane origin is equal to the total deformation of the bolt.

The Theory of Unsaturated Soil Mechanics

Bishop took the lead in proposing the shear strength expression of unsaturated soil in 1960:

$$\tau_f = c' + \left[(\sigma - u_a) + \chi (u_a - u_w) \right] \cdot \tan \phi' \quad (5)$$

where c' is the true cohesion; σ is the total stress; χ denotes a parameter related to the degree of saturation and the soil type; u_a represents the pore gas pressure; u_w is the porewater pressure; φ' is the effective internal friction angle. In the Bishop theory, the matrix suction $(u_a–u_w)$ is one part of effective stress, but the two vary in the action mechanism and should not be simply superposed. [15] In addition, it is difficult to determine the parameter χ, so this theory has been scarcely applied in practice.

Given the above problems, Fredlund et al. introduced suction, as an independent variable, into the theory of unsaturated soil mechanics in 1978, with its expression as below:

$$\tau_f = c' + (\sigma - u_a) \cdot \tan \phi' + (u_a - u_w) \tan \phi^b \quad (6)$$

where φ^b is a parameter related to the change in the matric suction; $\tan\varphi^b$ represents the increase in rate of shear strength with the matric suction.

Based on the above cognition, the Fredlund theory was mainly used in this study to derive and analyze the mechanical model subsequently. To simplify the analysis, the full length of the full-length binding-type anti-floating bolt was regarded as the anchorage section. For the anti-floating bolt, the interface between the anchoring body and soil mass (anchorage interface) is generally the interface most susceptible to the failure. In this case, the bearing capacity of the anti-floating bolt depends on the shear strength of the soil mass. Hence, τ_f in the Fredlund theory can be considered as a shear stress acting upon the bolt body and also the total shear stress acting upon the surrounding soil mass, which consists of three parts. The $(\sigma–u_a) \tan\varphi'$ term indicates the shear stress generated when the external load acts upon the soil skeleton and the main source causing the soil deformation. In general, the $(u_a–u_w) \tan\varphi_b$ term is the additional shear stress generated by the suction, considered as one part of the total cohesion of the soil mass, and can be referred to as the apparent cohesion. [14] Therefore, the Fredlund theory of unsaturated soil mechanics can be transformed into the following form:

$$\tau_f = c' + \tau + \tau_0 \quad (7)$$

$$\tau = (\sigma - u_a) \cdot \tan \phi' \quad (8)$$

$$\tau_0 = (u_a - u_w) \cdot \tan \phi^b \quad (9)$$

Establishment of Mechanical Model

If the bolt is divided into innumerable microelements along the depth direction, the schematic diagram of their stress conditions is displayed in Fig. 5. According to the equilibrium relationship of such microelements, the axial force $dP(z)$ on them can be expressed as:

$$dP(z) = -\pi D \cdot \tau_f(z) \cdot dz \tag{10}$$

where D denotes the bolt diameter.

According to the Hooke's law, the axial force and strain on the microelements conform to the following relationship:

$$P(z) = \frac{dW(z)}{dz} \cdot \frac{\pi D^2 E_a}{4} \tag{11}$$

where E_a represents the elastic modulus of the anchoring body.

Through the simultaneous Eqs. (10) and (11), the following can be obtained:

$$\frac{d^2 W(z)}{dz^2} + \frac{4}{D E_a} \tau_f(z) = 0 \tag{12}$$

Substituting Eq. (7) into (12), we obtain:

$$\frac{d^2 W(z)}{dz^2} + \frac{4}{D E_a} \left[c\prime + \tau(z) + \tau_0 \right] = 0 \tag{13}$$

According to Eq. (4), the displacement caused by $\tau(z)$ at O is:

$$dW(z) = \frac{D\tau(z)(3 - 2\mu)(1 + \mu)}{2Ez} \cdot dz \tag{14}$$

Substituting Eq. (14) into (13), we can acquire:

$$\frac{d^2 W(z)}{dz^2} + \frac{8Ez}{E_a D^2 (3 - 2\mu)(1 + \mu)} \cdot \frac{dW(z)}{dz} + \frac{4}{D E_a} \tau_0 + \frac{4}{D E_a} c' = 0 \tag{15}$$

Setting $A = \frac{8E}{E_a D^2 (3-2\mu)(1+\mu)}$ and $B = \frac{4}{D E_a} \tau_0 + \frac{4}{D E_a} c\prime$, Eq. (15) can be transformed into the following form:

$$\frac{d^2 W(z)}{dz^2} + A \cdot z \cdot \frac{dW(z)}{dz} + B = 0 \tag{16}$$

This equation is a non-homogeneous differential equation of the second-order variable coefficient, which is subjected to order reduction processing, thereby obtaining:

$$\frac{dW(z)}{dz} = -B e^{-\frac{1}{2}A z^2} \int e^{\frac{1}{2}A z^2} + C_1 e^{-\frac{1}{2}A z^2} \tag{17}$$

where C_1 is an undetermined constant.

This general solution contains transcendental functional integration that cannot be expressed by an elementary function, so it is expressed by means of power series expansion, and then Eq. (17) is changed into:

Fig. 5 Anchor bolt and microelement of anchor bolt force diagram
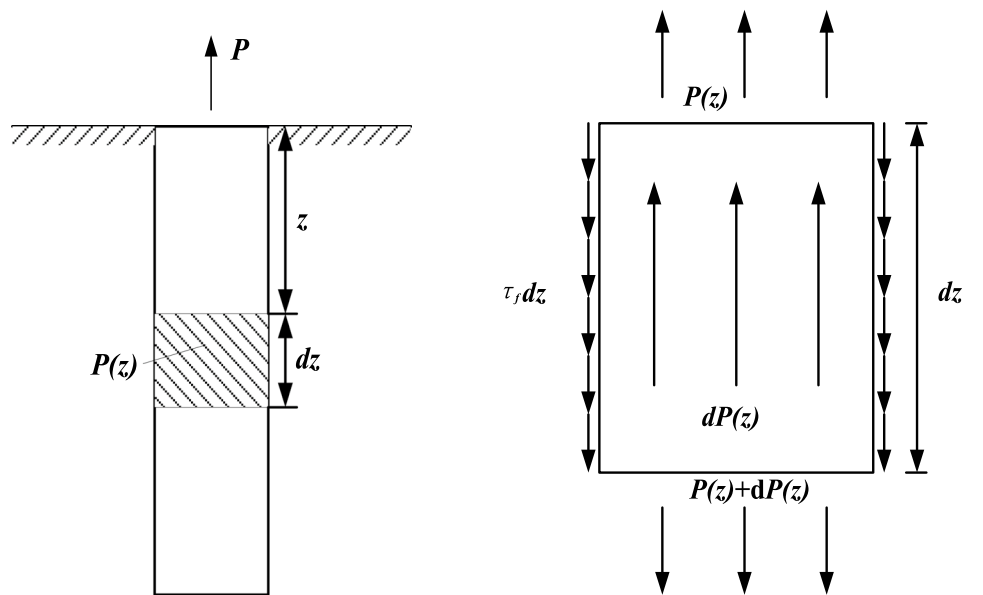
(a) Anchor bolt force diagram;   (b) Microelement of anchor bolt force diagram

$$\frac{dW(z)}{dz} = -B\,e^{-\frac{1}{2}Az^2} \cdot \left[\sum_{n=0}^{\infty} \frac{\left(\frac{1}{2}A\right)^n}{n!} \frac{1}{2n+1} z^{2n+1} \right] + C_1\,e^{-\frac{1}{2}Az^2}$$

$$= -B\,e^{-\frac{1}{2}Az^2} \cdot \left(z + \frac{1}{2}A\frac{1}{3}z^3 + \frac{1}{8}A^2\frac{1}{5}z^5 + \cdots \right) + C_1\,e^{-\frac{1}{2}Az^2} \tag{18}$$

Through the simultaneous Eqs. (18) and (11), $P(z) = P$ when the boundary condition is $z = 0$, and the distribution function of the axial force can be obtained as below:

$$P(z) = -\frac{\pi D^2 E_a}{4} B\,e^{-\frac{1}{2}Az^2} \cdot \left(z + \frac{1}{2}A\frac{1}{3}z^3 + \frac{1}{8}A^2\frac{1}{5}z^5 + \cdots \right)$$
$$+ P \cdot e^{-\frac{1}{2}Az^2} \tag{19}$$

where the undetermined constant is $C_1 = \frac{4P}{\pi D^2 E_a}$.

Through the simultaneous Eqs. (18) and (14), the distribution function of the shear stress can be obtained as follows:

$$\tau(z) = -\frac{D E_a}{4} ABz\,e^{-\frac{1}{2}Az^2} \cdot \left(z + \frac{1}{2}A\frac{1}{3}z^3 + \frac{1}{8}A^2\frac{1}{5}z^5 + \cdots \right)$$
$$+ \frac{AzP}{\pi D} \cdot e^{-\frac{1}{2}Az^2} \tag{20}$$

Equations (19) and (20) are power series solutions, and through analysis, the second terms in the two equations are consistent with the shear stress and axial force distribution functions of the anti-floating bolt in unsaturated soil based on the Mindlin solution, indicating that the first term in the two equations represents the influence of the matric suction on the shear stress and axial force.

Comparative Analysis of a Calculation Example

The design parameters for the anti-floating bolts in B2 of a commercial plaza in Northwest China are as follows: The design length of bolts is $l = 8.9$ m, the diameter and elastic modulus of the anchoring body are $D = 150$ mm and $E_a = 3 \times 10^4$ MPa, respectively, the surrounding soil layer is a silty-fine sand layer, the soil cohesion is $c' = 0$, the internal friction angle is $\varphi' = 36°$, and the Poisson's ratio and elastic modulus of the soil mass are $\mu = 0.25$ an $E = 40$ MPa, respectively. The maximum pull-out load was $P = 300$ kN in the single-bolt pull-out bearing capacity test. Since the precipitation operation was done in the foundation pit before the single-bolt pull-out bearing capacity test, the soil mass around the bolt was under an unsaturated state. In this study, an ultimate state was taken, namely, the degree of saturation of the surrounding soil mass was zero, the porewater pressure was then $u_w = 0$, the pore gas pressure was $u_a = 0.1$ MPa, and $\varphi_b = 33.3°$ was a constant. According to the Fredlund
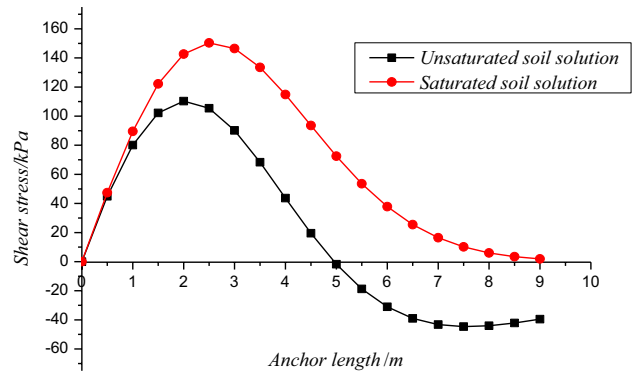

Fig. 6 Comparison of shear stress distribution curves of the full-length binding-type anti-floating bolt in unsaturated and saturated soil
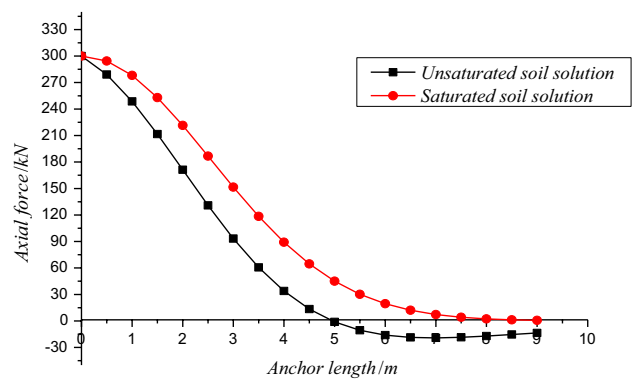

Fig. 7 Comparison of axial force distribution curves of the full-length binding-type anti-floating bolt in unsaturated and saturated soil

unsaturated soil theory, the additional shear stress generated by the matric suction was $\tau_0 = 0.066$ MPa. According to the above-calculated parameters, the shear stress and axial force distribution curve of the full-length binding-type anti-floating bolt in unsaturated soil were calculated using Eqs. (19) and (20) as shown in Figs. 6 and 7.

It could be known from Figs. 6 and 7 that the full-length binding-type anti-floating bolt in unsaturated soil presented the following stress characteristics:

(1) The shear stress was distributed along the full length of the bolt and became zero at the anchor bolt head. Then, as the depth increased, the shear stress firstly grew rapidly and then gradually declined, and the shear stress curve became a unimodal curve.

(2) For unsaturated soil, the shear stress reached the maximum value at the relative length of 0.2, and the saturated soil shear stress reached the maximum value at the relative length of 0.3. The unsaturated soil had a neutral point at the relative length of 0.5, and the shear stress below the neutral point was negative. The satu-

rated soil shear stress gradually declined to zero with the increase in the depth.

(3) The axial force was distributed along the full length of bolt and reached the maximum value at the anchor bolt head. As the depth increased, the axial force then gradually declined. The axial force of unsaturated soil decreases faster than that of saturated soil and decreases to zero at the relative length 0.5, and the axial force of unsaturated soil is negative. The axial force of saturated soil declined to zero at the relative depth of 0.9.

(4) Neutral points appeared in both the shear stress and axial force distributions of the anti-floating bolt in unsaturated soil, which was mainly attributed to the matric suction. Because of the matric suction, its pull-out bearing capacity was smaller than that of saturated soil, so the anti-floating bolt was unsafe if its pull-out resistance was determined according to the saturated soil theory.

Influencing Factor Analysis of Bearing Capacity Characteristics

In the design and construction of the anti-float bolt, there are many factors that combat the bearing capacity of the anti-float bolt, including the bolt characteristics, the soil characteristics, the load condition, the construction process, and so on. Due to the limited length, this section is only analyzed by the research content of this bolt. It could be known from Eqs. (19) and (20) that the bearing capacity of the full-length binding-type anti-float bolt in unsaturated soil is mainly influenced by the E_a、D、A and B value. The A and B value belongs to the intermediate parameter, and the value is also related to the true cohesion c, additional shear stress generated by the suction τ_0, and the soil body Poisson's ratio μ. The small number of the true cohesion c and the Poisson's ratio μ does not affect the shear strength of the bolt, and the additional shear stress τ_0 is the main feature of the unsaturated soil, so this paper focuses on the analysis of the influence factors of E_a, D, and τ_0.

Soil-Bolt Elastic Modulus Ratio E/E$_a$

E/E_a is the ratio of the soil mass's elastic modulus to the anchoring body's elastic modulus, and a greater E/E_a value indicates harder soil mass. Here, the influence of this ratio on the stress distribution of the anti-floating bolt in unsaturated soil was considered. The soil mass's elastic modulus E was set to 40, 50, 60, 70, and 80 MPa, respectively, while the anchoring body's elastic modulus was unchanged at $E_a = 3 \times 10^4$ MPa, and other design parameters were identical with those in the calculation example analysis in the preceding part. The shear stress and axial
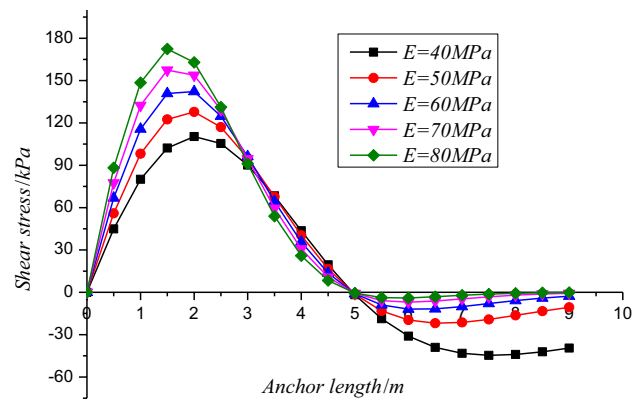

Fig. 8 Shear stress distribution curves of the full-length binding-type anti-floating bolt at different E/E_a values
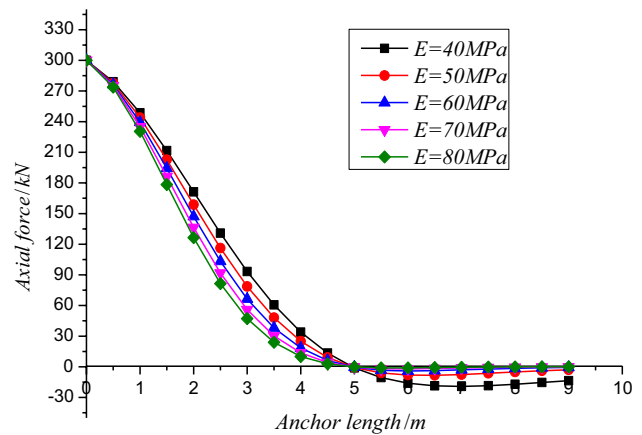

Fig. 9 Axial force distribution curves of the full-length binding-type anti-floating bolt at different E/E_a values

force distribution curves of the full-length binding-type anti-floating bolt at different E/E_a values are as shown in Figs. 8 and 9.

It could be known from Fig. 8 that the greater the soil mass's elastic modulus, the greater the E/E_a value, the greater the peak value of the shear stress curve, and the closer the peak value to the bolt hole. The position of the neutral point was not influenced by the E/E_a value, but as the E/E_a value increased, the negative shear stress after the neutral point was closer to zero.

As shown in Fig. 9, the greater the E/E_a value, the faster the axial force declined, but the maximum value of the axial force at the anchor bolt head was unchanged. The position of the neutral point of the axial force was not influenced by the E/E_a value, but as the E/E_a value increased, the negative axial force after the neutral point was closer to zero.
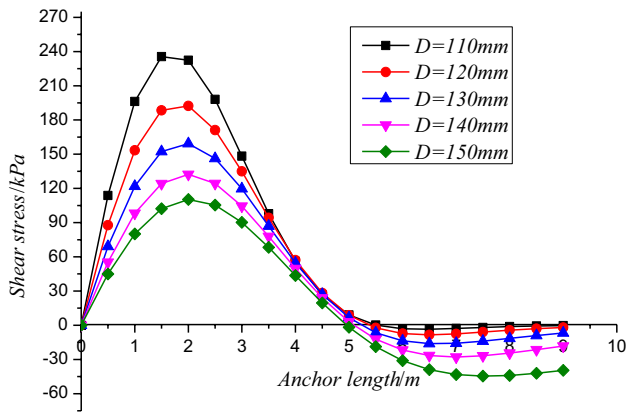
Fig. 10 Shear stress distribution curves of the full-length binding-type anti-floating bolt at different diameters D of the anchoring body
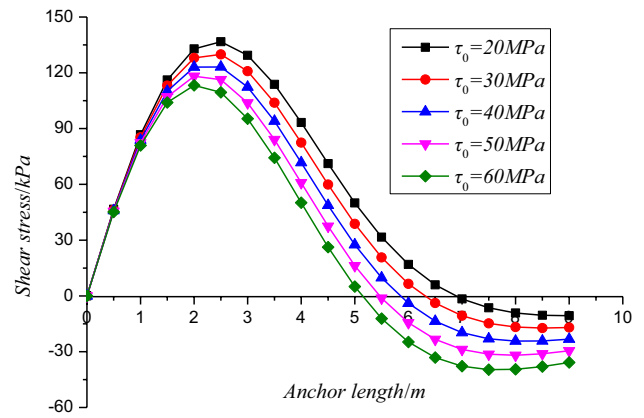

Fig. 12 Shear stress distribution curves of the full-length binding-type anti-floating bolt at different shear stresses τ_0
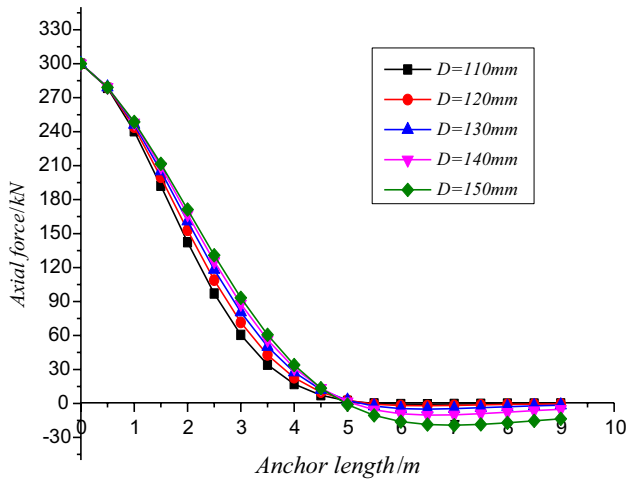

Fig. 11 Axial force distribution curves of the full-length binding-type anti-floating bolt at different diameters D of the anchoring body

Fig. 13 Axial force distribution curves of the full-length binding-type anti-floating bolt at different additional shear stresses τ_0

Diameter D of the Anchoring Body

Here, the influence of the diameter D of the anchoring body on the stress distribution of the anti-floating bolt in unsaturated soil was investigated. The diameter D of the anchoring body was set to 110, 120, 130, 140, and 150 mm, respectively, while the other design parameters were identical with those in the calculation example analysis in the preceding part. The shear stress and axial force distribution curves of the full-length binding-type anti-floating bolt at different diameters D of the anchoring body are exhibited in Figs. 10 and 11.

It could be known from Fig. 10 that as the diameter D of the anchoring body increased, the peak value of the shear stress declined and shifted backward, the neutral point moved forward, and the negative shear stress grew.
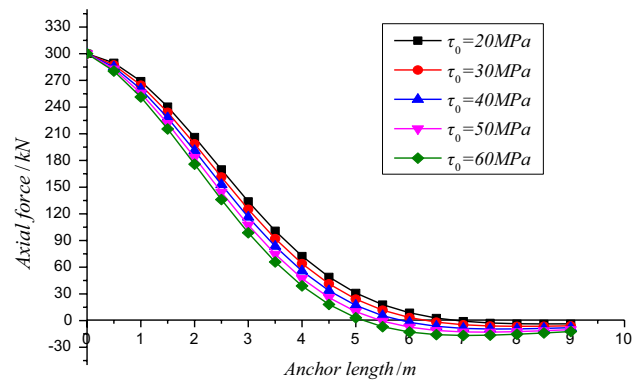
It could be known from Fig. 11 that at different diameters D of the anchoring body, the maximum axial force remained identical and did not influence the position of the neutral point. With the increase in the diameter D of the anchoring body, the reduction rate of the axial force distribution curve was reduced, but the negative axial force increased.

Additional Shear Stress τ_0

In this section, the influence of the additional shear stress τ_0 on the stress distribution of the anti-floating bolt in unsaturated soil was taken into account. The additional shear stress τ_0 was set to 20, 30, 40, 50, and 60 MPa, respectively, while the other design parameters were identical with the calculation example analysis in the preceding part. The shear stress and axial force distribution curves of the full-length binding-type anti-floating bolt at different additional shear stresses τ_0 are displayed in Figs. 12 and 13, respectively.

It could be observed from Fig. 12 that as the additional shear stress τ_0 increased, the peak value of the shear stress

curve declined and moved toward the anchor bolt head, the neutral point moved toward the porthole too, and the negative shear stress increased.

It could be known from Fig. 13 that at different additional shear stresses τ_0, the maximum axial force was the same. As the additional shear stress τ_0 increased, the reduction rate of the axial force distribution curve was accelerated, the neutral point moved toward the anchor bolt head, and the negative axial force grew.

Discussion

The conclusion obtained in this article is the result obtained under the limit state of zero pore water content. In practical engineering, unsaturated soils generally contain a certain amount of pore water, but the water content varies. The additional shear stress τ_0 of unsaturated soil is mainly influenced by the suction force (u_a–u_w). The moisture content of the soil layer decreases, the suction force and the additional shear stress gradually decrease, and the water content increases gradually when the groundwater is recovered. At present, the suction test technique cannot accurately determine the additional shear stress. According to the existing experimental work, the additional shear stress has a certain linear relationship with the pressure of the soil expansion, and the expansion pressure P_s is easily obtained through experiment; the relationship is:

$$\tau_0 = P_s \tan \phi \tag{21}$$

In Eq. (21), P_s is the swelling pressure, which refers to the vertical pressure required to maintain the volume of unsaturated soil samples under lateral confinement conditions when soaked in water. The φ is the internal friction angle of saturated soil.

In practical engineering, Eq. (21) can be applied to estimate additional shear stress, expanding the application range of the research content in this paper.

Conclusion

The theoretical solutions to the axial force and shear stress distributions of the full-length binding-type anti-floating bolt in unsaturated soil were derived based on the Mindlin solution and compared with the solutions to those in saturated soil. Moreover, the influences of various factors on the axial force and shear stress distributions were further discussed, and the following conclusions were drawn:

(1) The shear stress and axial force of the anti-floating bolt in unsaturated soil were distributed along the full length of the bolt, but neutral points appeared. This was mainly because the matric suction led to the axial force and shear stress reduction of the anti-floating bolt. If the anti-floating bolt was designed according to the solution of saturated soil, the anti-floating capacity of the bolt would be partially large.

(2) The larger the elastic modulus of soil, the larger the E/E_a value, the larger the peak value of shear stress curve, and the closer the peak value is to the anchor bolt head. The greater the value of E/E_a, the greater the rate of axial force decline. However, the positions of the neutral points for the axial force and shear stress were not influenced by the E/E_a value.

(3) As the diameter D of the anchoring body increased, the peak value of the shear stress declined and shifted backward, the neutral point moved forward and the negative shear stress grew. At different diameters D of the anchoring body, the maximum axial force was the same, and the position of the neutral point was not influenced. With the increase in the diameter D of the anchoring body, the reduction rate of axial force distribution curve was decelerated, but the negative axial force grew.

(4) As the additional shear stress τ_0 grew, the peak value of the shear stress curve declined and moved toward the anchor bolt head, the neutral point also moved toward the anchor bolt head, and the negative shear stress increased. At different additional shear stresses τ_0, the maximum axial force remained identical. With the increase in the additional shear stress τ_0, the reduction rate of the axial force distribution curve was accelerated, the neutral point moved toward the anchor bolt head, and the negative axial force grew.

May be in use, the research results of this paper in a few cases, in the case of very high uplift force, such as deep basement raft, in the "empty tank" under the condition of underground storage tanks, still need further research.

Data Availability The data used to support the findings of this study are available from the corresponding author upon request.

Declarations

Conflicts of interest The authors declare that they have no conflicts of interest.

References

1. Cheng-gang BAO (2004) Behavior of unsaturated soil and stability of expansive soil slope. Chin J Geotech Eng 01:1–15
2. Zheng-han CHEN (2014) On basic theories of unsaturated soils and special soils. Chin J Geotech Eng 36(02):201–272
3. Sun YL, Tang LS, Liu J (2020) Advances in research on microstructure and intergranular suction of unsaturated soils. Rock Soil Mech 41(04):1095–1122
4. Xiao-yu B, Hai-gang W, Ming-yi Z et al (2020) Research progress on bearing capacity of anti-floating anchor. Sci Technol Eng 20(8):2949–2958
5. Li JW, Qiao JG, Fu X, Liu XL et al (2019) Failure analysis of the anti-floating bolt system based on the fuzzy fault tree. J Safety Environ 19(04):1128–1134
6. Li D, Li Y, Zhu W (2020) Analytical modelling of load-displacement performance of cable bolts incorporating cracking propagation. Rock Mech Rock Eng 53(8):3471–3482
7. Xun M, Zheng-chao X, Qian Z et al (2022) Force analysis and application of full-length bonded anti-floating anchor. Archit Technol 53(06):745–748
8. De-sheng J, Xiao-yu B, Chao L et al (2021) Load-displacement characteristics and ultimate bearing capacity prediction of anti-floating anchor. Sci Technol Eng 21(22):9570–9576
9. Guomin L (2013) Research of Bearing capacity for Fully grouted Anchor in Highly-Moderately Weathered sandstone. Chengdu University of Technology.
10. Li D, Li Y, Chen J et al (2021) An analytical model for axial performance of rock bolts under constant confining pressure based on continuously yielding criterion. Tunn Undergr Space Technol 113:103955
11. Hui P, Chao Y, De-qiang X (2013) Distribution of stress on bonded length of tension-type rock bolt based on theory of elasticity. J Univ South China (Science and Technology) 27(04):100–104
12. Chunan Y (2000) Mechanical Analysis On Wholly Grouted Anchor. Chin J Rock Mech Eng 03:339–341
13. He JQ, Hu CB, Zhang JC (2012) Mechanical analysis of anchorage segment of pressure-type cable based on the Mindlin solution. Hydrogeol Eng Geol 39(01):47–52
14. Hong-zhou LIN, Guang-xin LI, Yu-zhen YU et al (2007) Influence of matric suction on shear strength behavior of unsaturated soils. Rock and Soil Mech 09:1931–1936
15. Zhao-jun L, Hui-ming Z, Jian-hua C et al (1992) Shear strength and swelling pressure of unsaturated soil. Chin J Geotech Eng 03:1–8